

Ultrafast X-Ray Diffraction Studies of the Phase Transitions and Equation of State of Scandium Shock Compressed to 82 GPa

R. Briggs, M. G. Gorman, A. L. Coleman, and R. S. McWilliams

SUPA, School of Physics and Astronomy, and Centre for Science at Extreme Conditions, The University of Edinburgh, Mayfield Road, Edinburgh EH9 3JZ, United Kingdom

E. E. McBride

European XFEL, Albert-Einstein-Ring 19, D-22761 Hamburg, Germany

D. McGonegle and J. S. Wark

Department of Physics, Clarendon Laboratory, Parks Road, University of Oxford, Oxford OX1 3PU, United Kingdom

L. Peacock and S. Rothman

Atomic Weapons Establishment, Aldermaston, Reading RG7 4PR, United Kingdom

S. G. Macleod

Atomic Weapons Establishment, Aldermaston, Reading, RG7 4PR, United Kingdom and Institute of Shock Physics, Imperial College London, SW7 2AZ, United Kingdom

C. A. Bolme and A. E. Gleason

Shock and Detonation Physics, Los Alamos National Laboratory, P.O. Box 1663, Los Alamos, New Mexico 87545, USA

G. W. Collins, J. H. Eggert, D. E. Fratanduono, and R. F. Smith

Lawrence Livermore National Laboratory, 6000 East Avenue, Livermore, California 94500, USA

E. Galtier, E. Granados, H. J. Lee, B. Nagler, I. Nam, and Z. Xing

Linac Coherent Light Source, SLAC National Accelerator Laboratory, Menlo Park, California 94025, USA

M. I. McMahon

SUPA, School of Physics and Astronomy, and Centre for Science at Extreme Conditions, The University of Edinburgh, Mayfield Road, Edinburgh, EH9 3JZ, United Kingdom and Research Complex at Harwell, Didcot, Oxon OX11 0FA, United Kingdom

(Received 22 January 2016; revised manuscript received 15 July 2016; published 9 January 2017)

Using x-ray diffraction at the Linac Coherent Light Source x-ray free-electron laser, we have determined simultaneously and self-consistently the phase transitions and equation of state (EOS) of the lightest transition metal, scandium, under shock compression. On compression scandium undergoes a structural phase transition between 32 and 35 GPa to the same bcc structure seen at high temperatures at ambient pressures, and then a further transition at 46 GPa to the incommensurate host-guest polymorph found above 21 GPa in static compression at room temperature. Shock melting of the host-guest phase is observed between 53 and 72 GPa with the disappearance of Bragg scattering and the growth of a broad asymmetric diffraction peak from the high-density liquid.

DOI: 10.1103/PhysRevLett.118.025501

The past 20 years have seen the discovery of a wealth of new and complex structures in the elements at high pressures [1], with perhaps the most outstanding examples being the incommensurate composite structures that comprise interpenetrating host and guest components [2]. Since their discovery in Ba [3], host-guest (HG) structures have been found in nine other elements, and are predicted to exist in aluminium at 3–5 TPa [4]. Such ultra-high-pressure states can be accessed routinely only via laser-compression techniques, but it is as yet unknown whether such complex

structures can form on the nanosecond time scales and at the high temperatures produced in such experiments.

One element with a high-pressure HG structure, which has been studied using both static and shock compression techniques, is scandium. At ambient conditions, Sc has the hcp structure (hcp-Sc), which on heating transforms to the bcc structure (bcc-Sc) at 1607 K, before melting at 1812 K [5]. On compression at 300 K, hcp-Sc transforms at 21 GPa [6] to a HG structure (HG-Sc) [7,8], which remains stable to 104 GPa [9].

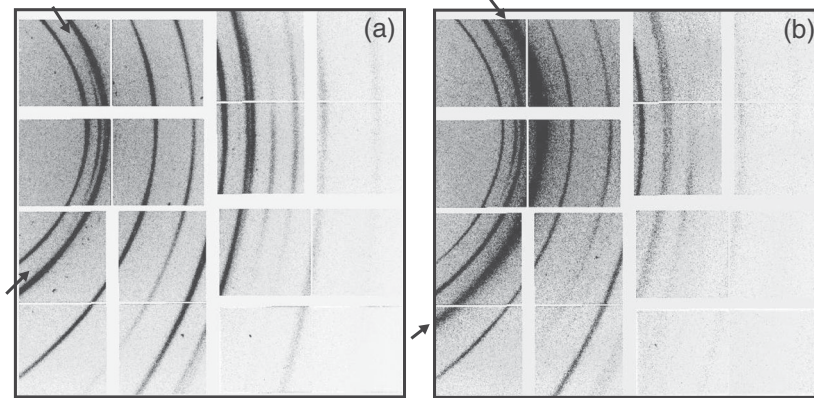


FIG. 1. 2D diffraction images collected on a single CSPAD detector from (a) uncompressed hcp-Sc and (b) Sc compressed to 51.1 GPa. The arrows in the two images highlight (a) the highly textured (002) Debye-Scherrer ring from uncompressed hcp-Sc and (b) the most intense Debye-Scherrer ring from the host-guest phase, the intensity distribution of which is much more uniform.

On the shock Hugoniot, the collection of states accessed by shock compression, a phase transition beginning at 16.5 GPa and completing by 38 GPa was identified from the deviation of existing shock Hugoniot data [10–12] from a calculated EOS for hcp-Sc and HG-Sc [13]; in the same study, *in situ* electrical measurements confirmed a transition. However, the earlier shock study by Carter *et al.* saw no evidence of a transition at 16.5 GPa, but saw a clear kink in $U_S - u_p$ (shock velocity—particle velocity) data at 35 GPa [12]. A phase transition to a further solid phase, or to the melt, was detected at 53 GPa [13]. Despite being unable to identify conclusively the phase transitions at 16.5, 35, and 53 GPa, since direct structural measurements were not available, the shock EOS of Sc is known to above 200 GPa [10–13].

To date, the measurement of an absolute EOS using laser-driven shock waves has been challenging, and reference to a standard EOS has generally been required. Furthermore, most modern laser-compression EOS data are reported on transparent materials, as an accurate and precise determination of the EOS of nontransparent materials, such as metals, poses major challenges. As a result, EOS data on opaque matter tend to exhibit considerable uncertainties, particularly in the density. However, the advent of x-ray free-electron lasers (XFELs) has resulted in an unprecedented improvement in the quality of diffraction data that can be obtained from dynamically compressed matter [14,15], making it possible to determine the crystal structure and density unambiguously with high precision. By combining such measurements with simultaneous velocimetry measurements, it is now possible to overcome previous limitations, and obtain EOS measurements without a reference, including for opaque materials.

Here we utilize x-ray diffraction at an XFEL to determine the EOS of scandium metal under shock compression and to study its structural evolution for direct comparison with prior isobaric heating and isothermal compression measurements. We observe a transition from hcp-Sc to bcc-Sc

between 32 and 35 GPa, a second transition at 46 GPa from bcc-Sc to HG-Sc, and then melting beginning at 53 GPa and being complete at 72 GPa.

Two experiments were performed at the MEC end station of the Linac Coherent Light Source (LCLS) [16]. A Nd:glass optical laser (527 nm, 20 ns quasiflattopped pulses) was used to launch an ablation-driven shock wave through the samples, which comprised a 50 μm thick polyimide ablator glued to 25 μm thick Sc foil of 99% purity. The LCLS provided quasimonochromatic ($\Delta E/E \sim 0.5\%$, $\lambda = 1.4089$ or 1.2400 \AA) x-ray pulses of 50 or 80 fs duration, each containing $\sim 10^{12}$ photons. The x-ray beam was focused to $50 \times 50 \mu\text{m}^2$ and then centered on the variable diameter focal spot of the drive laser, which, in turn, was centered on the target.

Two-dimensional diffraction images, as illustrated in Fig. 1, were recorded on multiple CSPAD detectors (Cornell-SLAC Pixel Array Detector) [17] placed in a transmission Debye-Scherrer geometry [18], which were then integrated azimuthally to produce 1D diffraction profiles. A velocity interferometer system for any reflector (VISAR) was used to both record the velocity-time histories of the rear free surface of the samples, thereby allowing the sample pressure to be determined, and to investigate any nonplanarity of the laser drive across the x-rayed region of the target.

The pressure was determined using the Rankine-Hugoniot equations from the measured densities and particle velocities, taken to be half the free-surface velocity [18]. In some cases, a LiF window was placed on the rear surface as a check on calculated pressures; in these cases, the pressure in the Sc was established from the value measured in the LiF [29] by impedance matching using prior Sc shock data [10–12]. Additional information on the experimental details and VISAR analysis is given in the Supplemental Material [18].

Data were collected between 0 and ~ 82 GPa, and contained clearly distinguishable diffraction patterns from

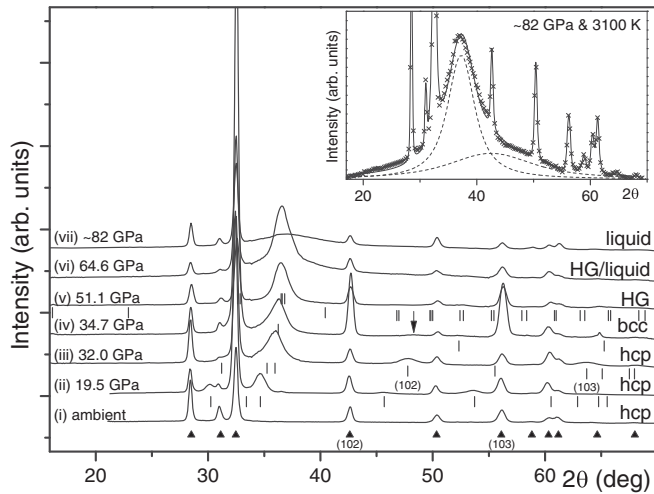


FIG. 2. Diffraction profiles from Sc on shock compression ($\lambda = 1.4089 \text{ \AA}$). The peaks from uncompressed hcp-Sc are identified by filled triangles below profile (i). The profiles show data from (i) uncompressed hcp-Sc; compressed hcp-Sc at (ii) 19.5 and (iii) 32.0 GPa; (iv) bcc-Sc at 35.6 GPa; (v) HG-Sc at 51.1 GPa; (vi) HG- and liquid-Sc at 64.6 GPa; and (vii) liquid-Sc at ~ 82 GPa. The peaks from the compressed hcp [profiles (ii) and (iii)], bcc [profile (iv)], and HG [profile (v)] phases are shown by tick marks beneath the profiles. The compressed hcp-Sc (102) and (103) reflections, the disappearance of which provides clear evidence of the hcp-to-bcc transition, are identified in profile (iii). A trace of the (102) peak is still observed at 34.7 GPa, as identified by the arrow in profile (iv). The inset shows an enlarged view of the ~ 82 GPa profile, where the asymmetry of the principal liquid peak is highlighted by fitting it with two Gaussians.

different solid phases and a liquid phase, as illustrated in Fig. 2. At pressures up to 32 GPa, only compressed hcp-Sc was observed, as identified from broadened hcp diffraction peaks displaced to higher angles; see profiles (ii) and (iii) in Fig. 2. Although the Debye-Scherrer rings from the compressed hcp-Sc are well defined and symmetric, they are both broader and noticeably less textured than those from the uncompressed material. This increased broadness and texture change is evident at all pressures, including data collected from samples compressed to only ~ 10 GPa which have undergone no phase transition, and is also present in samples released back to ambient pressure and arises from the many defects induced by the plastic deformation of the sample as it is strained beyond its elastic limit of ~ 0.4 GPa [28]. We have made a quantitative analysis of the microstress and grain size of the compressed samples, following the analysis conducted by Gleason *et al.* [23] in their shock compression study of quartz. We find that at 19.5 GPa, the grain size in compressed hcp-Sc is 25 (3) nm, considerably smaller than the measured grain size of 85(17) nm in the uncompressed Sc foil. The rms strain in the hcp-Sc phase at 19.5 GPa was measured to be less than $< 0.2\%$. Full details are given in the Supplemental Material [18].

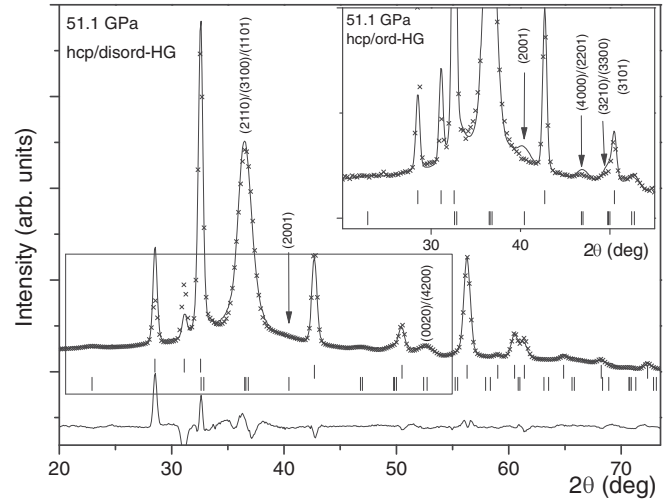


FIG. 3. A two-phase (62%:38% uncompressed-hcp:disordered-HG) Rietveld fit to the diffraction profile obtained at 51.1 GPa ($\lambda = 1.4089 \text{ \AA}$), with the most intense peaks indexed. The calculated peak positions of the best-fitting uncompressed-hcp and HG unit cells are shown by upper and lower tick marks beneath the profile. The inset shows an uncompressed-hcp:ordered-HG fit to the same profile. The additional (2001) guest-only peak, and the intensity mismatches caused by the intensities of the (2201) and (3101) guest-only peaks, are highlighted with arrows.

Between 32 and 35 GPa, Sc undergoes a phase transition, resulting in the disappearance of the (102) and (103) hcp reflection at $2\theta \sim 48^\circ$ and $\sim 64^\circ$, respectively, and the appearance of an intense diffraction peak at $2\theta = 36.2^\circ$ and a weaker peak at 52.2° [Fig. 2, profile (iv)]. The d -spacing ratio of these two peaks is $\sqrt{2}$, and they can thus be indexed as the (110) and (200) peaks of bcc-Sc with $a = 3.200 \text{ \AA}$ at 34.7 GPa ($V/V_0 = 0.657$). However, the same ratio relates the d spacings of the (2110)/(3100)/(1101) and (0020)/(4200) peaks of HG-Sc [30] with $a = 7.16 \text{ \AA}$, $c = 3.20 \text{ \AA}$, and $\gamma = 1.28$ ($V/V_0 = 0.621$), where γ is the incommensurate wave vector.

Closer analysis of our highest-quality diffraction pattern at 51.1 GPa [Fig. 2, profile (v), and Fig. 3] revealed the existence of two much weaker diffraction features at 46.9° and 49.8° , neither of which are accounted for by bcc-Sc. While both peaks are predicted by the HG phase, this structure would also predict a more intense peak—the (2001)—at 40.4° that should be clearly visible (see inset of Fig. 3). This is a ($hk0m$) “guest-only” peak, and arises from scattering from the chains of guest atoms only [30]. If these chains were disordered, as we have observed in HG-Rb at 300 K [31], and in HG-K at high temperatures [32], then this, and other, ($hk0m$) guest-only peaks would be extremely weak and not visible. A Rietveld refinement of the 51.1 GPa profile using a disordered HG model is shown in Fig. 3, and is excellent, accounting for all observed features. Indeed, the use of a disordered model also

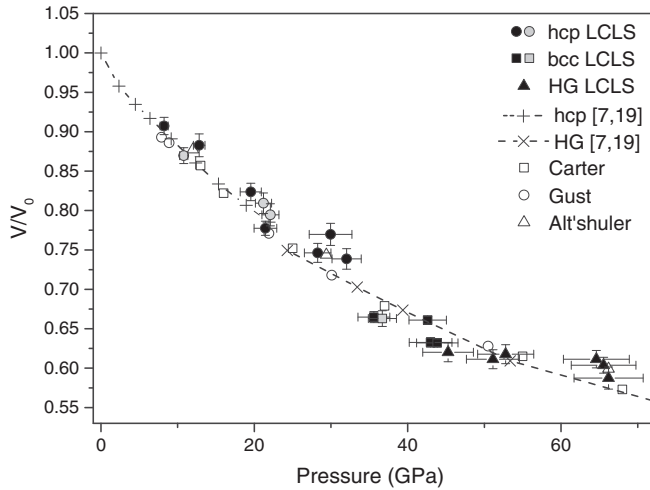


FIG. 4. Volumetric compression for Sc. Hugoniot EOS data obtained from this study are shown using filled black symbols, and points obtained using a LiF backing window are shown using filled gray symbols. The unfilled symbols show the previous shock compression data of Gust and Royce [11], Altshuler *et al.* [10], and Carter *et al.* [12]. The crosses and dashed lines show the corrected isothermal compressibility data at 300 K [7], assuming $\gamma = 1.280$ at all pressures for the HG phase [18].

improves the fit to the two peaks at 46.9° and 49.8° , both of which have an intensity contribution from $(hk0m)$ guest-only peaks, and are calculated to be more intense in an ordered structural model (Fig. 3, inset). The best fitting lattice parameters at 51.1 GPa are $a = 7.095(2)$ Å, $c = 3.190(1)$ Å, and $\gamma = 1.280$ (constrained to the value found at 300 K [31]). For comparison, the lattice parameters of ordered HG-Sc at 51 GPa and 300 K are $a = 7.18$ Å and $c = 3.18$ Å [7].

Fitting all diffraction data between 35 and 53 GPa to a HG structure led to an unphysically small compressibility, and poor agreement with previous shock data. Fitting the same data with bcc-Sc led to exactly the same problems. However, further analysis of the diffraction data revealed that there was no evidence of the weaker HG-Sc peaks below 45 GPa, and that between 35 and 45 GPa the data were completely accounted for by bcc-Sc. A Rietveld fit to an uncompressed-hcp:bcc profile at 35.0 GPa is shown in Fig. S4 of the Supplemental Material [18]. As the sample density calculated from a diffraction pattern differs by $\sim 3\%$ depending on whether one assumes it is bcc-Sc or HG-Sc (see above), calculating the densities between 35 and 45 GPa assuming bcc-Sc, and between 45 and 53 GPa assuming HG-Sc, resulted in both a physically sensible compressibility and good agreement with previous studies (Fig. 4). There is no evidence of any volume change at the bcc-HG transition.

Above 53 GPa we observe a clear increase in the background level in the vicinity of the most intense HG diffraction peak [Fig. 2, profile (vi)], which we attribute to

the first appearance of scattering from liquid-Sc. The observation of incipient melting at 53 GPa is in perfect agreement with the report of a phase transformation at 53 GPa by Molodets *et al.* [13]. The melting temperature is estimated from the shock temperature of the solid at 53 GPa to be ~ 2200 K [11].

As the sample pressure was increased above 53 GPa, the intense HG diffraction peak reduced in intensity, and disappeared at 72 GPa, above which only diffraction from liquid-Sc was observed [Fig. 2, profile (vii)]. This melting behavior suggests that the shock Hugoniot follows the Sc melting curve from 53 to 72 GPa before wholly entering the liquid phase. This agrees with one of the interpretations of Molodet *et al.* of their own data, where a mixed solid-liquid region is found between 53 and 72 GPa. The diffraction peak from the liquid is very distinctive, with a width that is 4–5 times that of the peak from HG-Sc [compare profiles (vi) and (vii) in Fig. 2], and is asymmetric (see inset of Fig. 2). Such an asymmetry suggests that Sc is not a simple liquid under such conditions [33–35].

Above 72 GPa, the free surface became entirely non-reflecting upon shock breakout, as is commonly observed as a consequence of melting and consistent with total melting above this pressure. Extrapolation of the liquid-diffraction peak position versus pressure [18] suggests that our highest-pressure liquid diffraction profile was obtained at ~ 82 GPa and 3100 K. The liquid diffraction data at this maximum pressure (see Fig. 2 inset) exhibits a high signal-to-noise ratio, and the diffraction profile contains scattering from only liquid-Sc and uncompressed hcp-Sc. While the q range of the data is limited by both the relatively long x-ray wavelengths used in this study and the limited angular coverage of the CSPAD detectors, the signal-to-noise ratio is perhaps better than that obtainable from a laser-heated diamond anvil cell (LHDAC) at the same $P - T$ conditions. The LCLS data also contain scattering only from the sample, and are free of parasitic scattering from the thermally insulating materials that typically encase the sample in a LHDAC experiment [36,37]. The LCLS liquid data are also free of diffraction peaks from contaminants, such as oxides and carbides, that can form as a result of extended laser heating in a DAC [38].

The phase diagram of Sc to 90 GPa and 3500 K obtained from our data is shown in Fig. 5. The Hugoniot shown is that of hcp-Sc [39]—a multi-solid-phase EOS for Sc is not yet available. The initial gradient of the hcp-HG phase boundary was confirmed in a high-pressure high-temperature static compression experiment at a synchrotron [18], and the phase transition points are shown. Up to 900 K, the HG-Sc was found to have ordered guest chains. The observation of a phase transition to bcc-Sc between 32 and 35 GPa along the Hugoniot is in excellent agreement with the transition reported in previous shock studies [12,13], while the lack of any volume change at the bcc-to-HG transition at 46 GPa probably prevented its detection in previous nondiffraction studies.

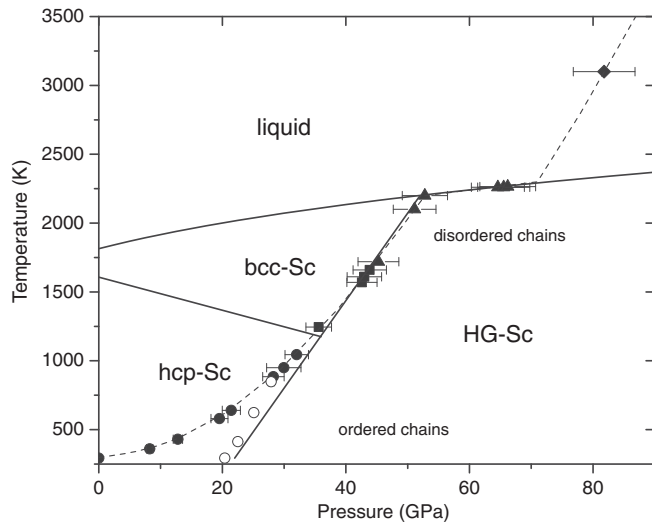


FIG. 5. The proposed phase diagram of Sc to 90 GPa and 3500 K. The short-dashed line shows the calculated hcp-Sc Hugoniot [39], a multiphase Hugoniot is not yet available, while the melt curve is a Simon-Glatzel fit to the ambient-pressure melting temperature and that at 53 GPa. Proposed phase boundaries between the hcp, bcc, and HG phases are shown with solid lines. The unfilled circles show the hcp-HG phase boundary, as determined in our static compression experiment.

The observation of the incommensurate HG structure of Sc is an important step in understanding the behavior of matter under shock compression. Not only is this complex incommensurate equilibrium phase formed on the subnanosecond time scales associated with laser-compression experiments, and observed up to 53 GPa and 2200 K, but the quality of the data obtained at the LCLS is sufficient to determine that the structure has undergone sublattice melting, as previously seen in other HG phases [31,32].

We believe this work represents an important benchmark on the path towards accurate EOS measurements in laser-driven dynamic compression experiments, particularly for opaque materials. The clarity with which both shock-induced solid-solid phase transitions and incipient or complete melting can be observed and distinguished in a relatively low- Z element like Sc ($Z = 21$) to 82 GPa holds great promise for future XFEL studies of similar phenomena in other materials to higher pressures. The quality and q range of the liquid diffraction data are almost sufficient to obtain a radial distribution function via Fourier transform of the diffraction profile. Unfortunately, the data extend to only $q = 5.5 \text{ \AA}^{-1}$, slightly too low to be analyzable via a Fourier transform. However, by increasing the energy of the x rays, and moving the detectors to obtain greater angular coverage, the q range can be extended to $\sim 8 \text{ \AA}^{-1}$, which simulations show is a sufficient range to obtain a quantitative radial distribution function sufficient to extend diffraction density measurements beyond the solid state. Obtaining such information from liquids at P - T conditions beyond those accessible with laser-heated DACs opens

exciting possibilities for the study of liquids at planetary-core conditions.

In conclusion, by combining diffraction and velocimetry measurements, we have eliminated numerous uncertainties in the compression behavior of scandium, thereby showing the significant value of combining measurements of phase and equation of state to definitively interpret the dynamic compression response of materials.

M. I. M. and J. S. W. would like to acknowledge support from EPSRC under Grants No. EP/J017256/1 and No. EP/J017051/1. D. M. is supported by LLNS under Contract No. B595954. E. E. M. acknowledges funding from the VolkswagenStiftung. The work by J. H. E., D. E. F., R. F. S., and G. W. C. was performed under the auspices of the U.S. Department of Energy by Lawrence Livermore National Laboratory under Contract No. DE-AC52-07NA27344. C. A. B. would like to acknowledge support from Science Campaign 2 at Los Alamos National Laboratory, which is operated for the National Nuclear Security Administration of the U.S. Department of Energy under Contract No. DE-AC52-06NA25396. Use of the Linac Coherent Light Source (LCLS), SLAC National Accelerator Laboratory, is supported by the U.S. Department of Energy, Office of Science, Office of Basic Energy Sciences under Contract No. DE-AC02-76SF00515. The MEC instrument is supported by the U.S. Department of Energy, Office of Science, Office of Fusion Energy Sciences under Contract No. SF00515. We would like to thank Carol A. Davis of LLNL for her help in preparing the Sc targets, and Dr Giulia De Lorenzi-Venneri of LANL for supplying the Sc EOS used in Fig. 5. We thank Diamond Light Source (DLS) for provision of synchrotron time and support, and thank Craig Wilson and Dominik Daisenberger of DLS for their help with the experiment.

-
- [1] M. I. McMahon and R. J. Nelmes, *Chem. Soc. Rev.* **35**, 943 (2006).
 - [2] M. McMahon and R. Nelmes, *Z. Kristallogr.* **219**, 742 (2004).
 - [3] R. J. Nelmes, D. R. Allan, M. I. McMahon, and S. A. Belmonte, *Phys. Rev. Lett.* **83**, 4081 (1999).
 - [4] C. J. Pickard and R. J. Needs, *Nat. Mater.* **9**, 624 (2010).
 - [5] B. J. Beaudry and A. H. Daane, *Trans. Metall. Soc. AIME* **224**, 770 (1962).
 - [6] Y. K. Vohra, W. Grosshans, and W. B. Holzapfel, *Phys. Rev. B* **25**, 6019 (1982).
 - [7] H. Fujihisa, Y. Akahama, H. Kawamura, Y. Gotoh, H. Yamawaki, M. Sakashita, S. Takeya, and K. Honda, *Phys. Rev. B* **72**, 132103 (2005).
 - [8] M. I. McMahon, L. F. Lundegaard, C. Hejny, S. Falconi, and R. J. Nelmes, *Phys. Rev. B* **73**, 134102 (2006).
 - [9] Y. Akahama, H. Fujihisa, and H. Kawamura, *Phys. Rev. Lett.* **94**, 195503 (2005).

- [10] L. V. Altshuler, A. A. Bakanova, and I. P. Dudoladov, *Sov. Phys. JETP* **26**, 1115 (1968).
- [11] W. H. Gust and E. B. Royce, *Phys. Rev. B* **8**, 3595 (1973).
- [12] W. J. Carter, J. N. Fritz, S. P. Marsh, and R. G. McQueen, *J. Phys. Chem. Solids* **36**, 741 (1975).
- [13] A. M. Molodets, D. V. Shakhrya, A. A. Golyshev, and V. E. Fortov, *Phys. Rev. B* **75**, 224111 (2007).
- [14] L. B. Fletcher, H. J. Lee, T. Doepfner, E. Galtier, B. Nagler, P. Heimann, C. Fortmann, S. LePape, T. Ma, M. Millot *et al.*, *Nat. Photonics* **9**, 274 (2015).
- [15] M. G. Gorman, R. Briggs, E. E. McBride, A. Higginbotham, B. Arnold, J. H. Eggert, D. E. Fratanduono, E. Galtier, A. E. Lazicki, H. J. Lee *et al.*, *Phys. Rev. Lett.* **115**, 095701 (2015).
- [16] B. Nagler, B. Arnold, G. Bouchard, R. F. Boyce, R. M. Boyce, A. Callen, M. Campell, R. Curiel, E. Galtier, J. Garofoli *et al.*, *J. Synchrotron Radiat.* **22**, 520 (2015).
- [17] P. Hart, S. Boutet, G. Carini, M. Dubrovin, B. Duda, D. Fritz, G. Haller, R. Herbst, S. Herrmann, C. Kenney *et al.*, *Proc. SPIE Proc.* **8504**, 85040C (2012).
- [18] See Supplemental Material at <http://link.aps.org/supplemental/10.1103/PhysRevLett.118.025501> for additional information on the experiments, pressure determination in the liquid, and corrections to the previous static compression data, which includes Refs. [19–28].
- [19] P. M. Celliers, D. K. Bradley, G. W. Collins, D. G. Hicks, T. R. Boehly, and W. J. Armstrong, *Rev. Sci. Instrum.* **75**, 4916 (2004).
- [20] J. W. Forbes, *Shockwave Compression of Condensed Matter* (Springer, New York, 2012).
- [21] B. Warren and B. Averbach, *J. Appl. Phys.* **21**, 595 (1950).
- [22] J. A. Hawreliak, D. H. Kalantar, J. S. Stolken, B. A. Remington, H. E. Lorenzana, and J. S. Wark, *Phys. Rev. B* **78**, 220101 (2008).
- [23] A. E. Gleason, C. A. Bolme, H. J. Lee, B. Nagler, E. Galtier, D. Milathianaki, J. Hawreliak, R. G. Kraus, J. H. Eggert, D. E. Fratanduono, G. W. Collins, R. Sandberg, W. Yang and W. L. Mao, *Nat. Commun.* **6**, 8191 (2015).
- [24] <https://www-s.nist.gov/srmors/certificates/674b.pdf>.
- [25] A. P. Hammersley, S. O. Svensson, M. Hanfland, A. N. Fitch, and D. Häusermann, *High Press. Res.* **14**, 235 (1996).
- [26] L. M. Barker and R. E. Hollenbach, *J. Appl. Phys.* **45**, 4872 (1974).
- [27] P. M. Celliers, G. W. Collins, D. G. Hicks, and J. H. Eggert, *J. Appl. Phys.* **98**, 113529 (2005).
- [28] D. Geiselman, *J. Less-Common Met.* **4**, 362 (1962).
- [29] D. Hayes, *J. Appl. Phys.* **89**, 6484 (2001).
- [30] The Miller indices used to identify reflections from host-guest structures are of the form $(hklm)$. Reflections from the host component of the basic composite structure have indices $(hkl0)$, those from the guest have indices $(hk0m)$, and the $(hk00)$ reflections are common to both host and guest. Interactions between the host and guest will result in shifts with respect to the lattice periodic atomic positions, giving rise to extremely weak satellite reflections $(hklm)$ with both l and $m \neq 0$. These have been omitted from the refinements conducted here.
- [31] M. I. McMahon and R. J. Nelmes, *Phys. Rev. Lett.* **93**, 055501 (2004).
- [32] E. E. McBride, K. A. Munro, G. W. Stinton, R. J. Husband, R. Briggs, H. P. Liermann, and M. I. McMahon, *Phys. Rev. B* **91**, 144111 (2015).
- [33] J. P. Hansen and I. R. McDonald, *Theory of Simple Liquids* (Academic Press, London, 1990).
- [34] N. W. Ashcroft and J. Lekner, *Phys. Rev.* **145**, 83 (1966).
- [35] G. Shen, V. B. Prakapenka, M. L. Rivers, and S. R. Sutton, *Phys. Rev. Lett.* **92**, 185701 (2004).
- [36] A. Cadien, Q. Y. Hu, Y. Meng, Y. Q. Cheng, M. W. Chen, J. F. Shu, H. K. Mao, and H. W. Sheng, *Phys. Rev. Lett.* **110**, 125503 (2013).
- [37] S. Anzellini, A. Dewaele, M. Mezouar, P. Loubeyre, and G. Morard, *Science* **340**, 464 (2013).
- [38] A. Dewaele, M. Mezouar, N. Guignot, and P. Loubeyre, *Phys. Rev. Lett.* **104**, 255701 (2010).
- [39] G. De Lorenzi-Venneri, Los Alamos National Laboratory, Technical Report No. LA-UR-12-25498.